Fizika Nizkikh Temperatur, 2005, v. 31, Nos. 8/9, p. 952–967

Ordering in two-dimensional Ising models with competing interactions

Gennady Y. Chitov

Department 7.1-Theoretical Physics, University of Saarland, Saarbrücken D-66041, Germany
Department of Physics and Astronomy, Laurentian University, Sudbury, ON, P3E 2C6 Canada
E-mail: gchitov@laurentian.ca

Claudius Gros

Department 7.1-Theoretical Physics, University of Saarland, Saarbrücken D-66041, Germany
Institute for Theoretical Physics, Frankfurt University, Frankfurt 60438, Germany

Received February 28, 2005

We study the 2D Ising model on a square lattice with additional non-equal diagonal next-nearest neighbor interactions. The cases of classical and quantum (transverse) models are considered. Possible phases and their locations in the space of three Ising couplings are analyzed. In particular, incommensurate phases occurring only at non-equal diagonal couplings, are predicted. We also analyze a spin-pseudospin model comprised of the quantum Ising model coupled to *XY* spin chains in a particular region of interactions, corresponding to the Ising sector's super-antiferromagnetic (SAF) ground state. The spin-SAF transition in the coupled Ising-XY model into a phase with co-existent SAF Ising (pseudospin) long-range order and a spin gap is considered. Along with destruction of the quantum critical point of the Ising sector, the phase diagram of the Ising-XY model can also demonstrate a re-entrance of the spin-SAF phase. A detailed study of the latter is presented. The mechanism of the re-entrance, due to interplay of interactions in the coupled model, and the conditions of its appearance are established. Applications of the spin-SAF theory for the transition in the quarter-filled ladder compound NaV_2O_5 are discussed.

PACS: 71.10.Fd, 71.10.Hf, 75.30.Et, **64.60.–i**

1. Introduction

The role of competing interactions in ordering is a fascinating problem of condensed matter physics. One of the most canonical examples of such systems are frustrated Ising models which demonstrate a plethora of critical properties, far from being exhaustively studied. (For a review see [1].) The frustrations* can be either geometrical, like, e.g., in the Ising model on a triangular lattice, or they can be brought about by the next-nearest neighbor (NNN) interactions. Competing interactions (frustrations) can, e.g., result in new phases, change the Ising universality class, or even destroy the order at all. Another interesting aspect of the criticality in frustrated Ising models is an appearance of quantum critical point(s) (QCP) at special frustration points of model's high degeneracy, and related quantum phase transitions [2].

Inclusion of a transverse field (Ω) brings an extra scale into the game, giving raise to a new and complicated critical behavior. The Ising models with $\Omega = 0$ and $\Omega \neq 0$ are also often called classical and quantum, respectively. For a review on the Ising models in transverse field (IMTF) see [3]. Most studies of the frustrated quantum Ising models are restricted to their ground states properties, when mapping of the d-dimensional quantum model at $T = 0$ onto its $(d + 1)$-dimensional classical counterpart helps to analyze the

* We use the term «frustration» in a broad sense [1], meaning only that there is no spin arrangement on an elementary plaquette which can satisfy all bonds.

ground state phase diagram of the former. For the NNN 2D models we are interested in, there has been a considerable effort on the quantum anisotropic NNN Ising (ANNNI) model, reviewed in [3]. The studies of some other 2D frustrated transverse Ising models have appeared only recently [4,5].

Our interest in the subject comes from the earlier work on a quantum Ising model coupled to the spin chains [6]. This kind of coupled so-called spin-pseudospin (or spin-orbital) models appear in context of the phase transition in NaV_2O_5, which has inspired a great experimental and theoretical effort in recent years. (For a review see [7].) Going deeper into analysis, we came to realize that the Ising sector of the problem is in fact the 2D transverse NN and NNN Ising model on a square lattice. It turns out that even its classical counterpart ($\Omega = 0$) was studied only for the case of equal NNN couplings $J_1 = J_2$ [1]. The elementary plaquette of this lattice with the notations for couplings is shown in Fig. 1. To the best of our knowledge, this 2D NN and NNN Ising model in transverse field is a complete *terra incognita* even at $J_1 = J_2$.

So, as the first step, we find the ground state phase diagram of the classical ($\Omega = 0$) Ising model at arbitrary couplings $J_\square, J_1, J_2$. Along with the three ordered phases found earlier by Fan and Wu [8] for the case $J_1 = J_2$ — ferromagnetic (FM), antiferromagnetic (AF), and super-antiferromagnetic (SAF) — the model has a fourth phase which can occur if sign $(J_1/J_2) = -1$. We call it super-ferro-antiferromagnetic (SFAF) [9]. From mean-field-type arguments we predict also the existence of an incommensurate (IC) phase at $T > 0$ in this model. The 2D IC phase is also called floating [10]. Similar phase is known for the well-studied 2D ANNNI model [1,10,11]. We present a qualitative temperature phase diagram for the regions of the coupling space where the IC phase is located. Note that the three phases — SAF, SFAF, IC — can occur only in the presence of competing interactions in the Ising model, and the latter two occur only if $J_1 \neq J_2$.

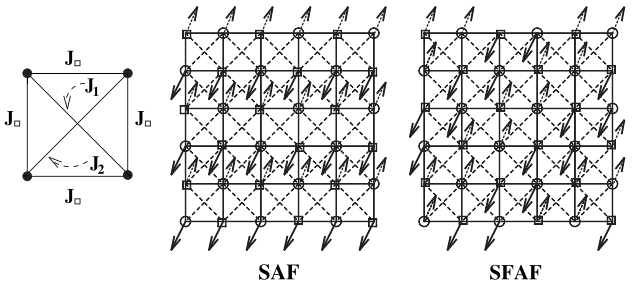

Fig. 1. Couplings on an elementary plaquette in the NN and NNN 2D Ising model (1). Ordering patterns in the super-antiferromagnetic (SAF) and super-ferro-antiferromagnetic (SFAF) phases.

This analysis of the classical Ising model lays the grounds for venturing into its study in presence of a transverse field. The role of transverse field is subtle. A more straightforward aspect is that its increase above certain critical value can eventually destroy the ordered state of the classical model, and in the ground state the transverse field results in appearance of a QCP. This is similar to the well-understood quantum NN Ising model. Another particularly interesting aspect in the role of transverse field is that it can lift degeneracy of the ground state and stabilize new phases at finite temperature in a highly frustrated model, like, e.g., the antiferromagnetic isotropic triangular Ising model [4,5], which is disordered at any $T > 0$ when $\Omega = 0$.

The behavior of the systems with infinitely degenerated ground states (with or without a finite ground-state entropy per spin) can be quite complicated in the presence of transverse field. It lies beyond the scope of the present work, and definitely cannot be understood from the mean-field analysis we apply in this study. For the NN and NNN Ising model we only identify the lines (planes) in the space of couplings $(J_\square, J_1, J_2)$ where the model is highly degenerated, and in their neighborhood we expect some new exotic phases generated by $\Omega \neq 0$ to appear.

From mapping of the NN and NNN IMTF at $T = 0$ onto its classical 3D counterpart, we qualitatively predict the (mean-field) ground-state phase boundaries of the quantum model in the coupling space $(J_\square, J_1, J_2)$. In particular, it follows from our analysis that in the presence of transverse field the IC ground-state phase can penetrate into some parts of the FM, AF, SAF regions of the classical model ($\Omega = 0$).

Finally, we consider the coupled spin-pseudospin model. It is proposed to analyze the transition in NaV_2O_5. This material provides a unique example of a correlated electron system, where the interplay of charge and spin degrees of freedom results in a phase transition into a phase with coexistent spin gap and charge order. NaV_2O_5 is the only known so far quarter-filled ladder compound. Each individual rung of a ladder is occupied by single electron which is equally distributed between its left/right sites in the disordered phase. At $T_c = 34$ K this compound undergoes a phase transition when a spin gap opens, accompanied by charge ordering [7].

The problem of the electrons in NaV_2O_5 localized on the rungs of the 2D array of ladders is mapped onto the coupled spin-pseudospin model on the effective

square lattice. The Ising sector of this model is given by the Hamiltonian of the NN and NNN IMTF, and the Ising variables (called pseudospins for this case) represent physically the charge degrees of freedom. We model the spin sector by the array of the XY spin chains. The 2D long-range charge order in NaV_2O_5 is identified as the SAF phase of the Ising model, and we restrict our analysis to the SAF region of the couplings $(J_\square, J_1, J_2)$. The coupled model is handled by combining the mean-field treatment of its Ising sector with the use of exact results available for the XY spin chains. Since the SAF state is only four-fold degenerated, the mean-field predictions for the Ising sector of the coupled model are expected to be at least qualitatively correct.

The mean-field equations for the coupled model are, with some minor modifications, the same as we have obtained earlier [6]. A striking feature of the coupled model is that it *always* orders from the charge-disordered spin-gapless state into the phase of co-existent SAF charge order and spin gap. We call this the spin-SAF transition. By *always* we mean that the critical temperature of the spin-SAF transition is non-zero for all Ising couplings within the whole considered SAF region. In other words, the QCP of the IMTF is destroyed, and this is due to the spin-charge (-pseudospin) coupling. This property of the spin-SAF transition and the parameters of the spin-SAF phase were studied earlier [6], so in this work we only reinstate some points and stress the distinctions pertinent to the present model.

The other remarkable feature of the coupled model's phase diagram is re-entrance, which was not well understood in our earlier work [6]. Now we carry out an analytical study of the re-entrance and establish the conditions when it can occur. This analysis allows us to understand the detailed mechanism of this interesting phenomenon generated by competing interactions.

The rest of the paper is organized as follows. Section 2 contains our results on the ordering in the 2D NN and NNN Ising model at $\Omega = 0$ and $\Omega \neq 0$. The results on the spin-SAF transition in the coupled model are presented in Sec. 3. The final Sec. 4 presents the summary and discussion.

2. 2D nearest- and next-nearest-neighbor Ising model

We consider the 2D Ising model on a square lattice with the Hamiltonian

$$H = \frac{1}{2}\sum_{\langle \mathbf{i},\mathbf{j}\rangle} J_\square \tau_{\mathbf{i}}^x \tau_{\mathbf{j}}^x + \frac{1}{2}\sum_{\langle\langle \mathbf{k},\mathbf{l}\rangle\rangle} J_{\mathbf{kl}} \tau_{\mathbf{k}}^x \tau_{\mathbf{l}}^x \ , \qquad (1)$$

where the bold variables denote lattice vectors, the first (second) sum includes only nearest neighbors (next-nearest neighbors) of the lattice, respectively. Spins along the sides of an elementary plaquette interact via the NN coupling $J_\square$, while spins along plaquette's diagonals interact via the NNN couplings $J_{\mathbf{kl}} = J_{1,2}$ (see Fig. 1). The way we defined the Hamiltonian corresponds to antiferromagnetic couplings for $J_\sharp > 0$ and ferromagnetic for $J_\sharp < 0$.

Ground state phases

There is no exact solution of the model (1). Its possible ordered phases and critical properties have been studied within various approaches for equal diagonal couplings $J_1 = J_2$ (see [1] for a review and references on the original literature). We will consider arbitrary Ising couplings $(J_1, J_2, J_\square)$, so the model (1) can be either frustrated or not (see footnote on the first page of this article). The ground state phase diagram can be found from energy arguments, as was first done by Fan and Wu for $J_1 = J_2$ [8]. (Their phase diagram is shown in Fig. 3,*c*.) From direct counting of the ground state energies of possible spin arrangements we construct the phase diagram for $J_1 \neq J_2$. Along with the phases found by Fan and Wu — ferromagnetic, antiferromagnetic, and super-antiferromagnetic — there is a fourth phase which can occur if J_1 and J_2 have opposite signs. The name of the SAF phase comes from viewing it as two superimposed antiferromagnetic lattices (one lattice of circled sites and another of squared sites in Fig. 1). In the SAF state there are two frustrated bonds $J_\square$ per plaquette and its energy is four-fold degenerate, since each of the superimposed lattices can be flipped independently. In addition to the two SAF states with alternating ferromagnetic order along the horizontal chains (one of these is shown in Fig. 1), there are two states with the vertical ferromagnetic order.

The new fourth phase shown in Fig. 1 can be viewed as two superimposed lattices each of which is ordered ferromagnetically along one side (e.g., $J_2 < 0$) and antiferromagnetically along the other (e.g., $J_1 > 0$). So we will call it super-ferro-antiferromagnetic (SFAF) [9]. The SFAF state also has two frustrated plaquette's bonds and four-fold degeneracy. The ordering pattern shown in Fig. 1 changes only by a lattice spacing shift over flipping of the sublattices. The direction of the ferromagnetic order is determined by the ferromagnetic diagonal.

The ground state phases in the space $(J_1, J_2, J_\square)$ are shown in Fig. 2. In order to facilitate perception of this picture, we also present in Figs. 3, 4 several plane projections of the 3D Fig. 2. In the first quadrant

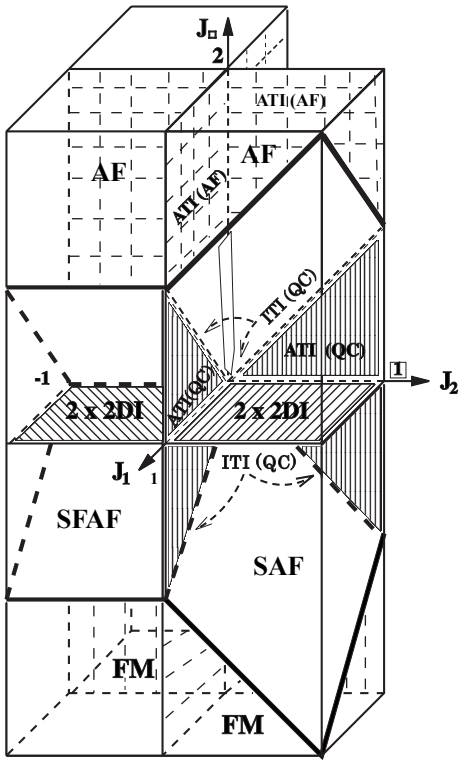

Fig. 2. Phase diagram of the ground states (GS) of the model (1). For visualization purposes it is drawn within $(-1,1)\times(-1,1)\times(-2,2)$ parallelepiped. The SAF GS lies between the frustration planes $J_1 + J_2 = |J_\square|$. The SFAF GS lies between the frustration planes $J_1 = |J_\square|$. The AF GS (FM GS) lies above (beneath) the frustration planes and above (beneath) the basal plane in the third quadrant, respectively. The second quadrant (not shown) is obtained by a reflection over $J_1 = J_2$ plane. Different sectors shown by hatched and twiggy lines on the exactly-solvable planes $J_\sharp = 0$ are explained in the text.

$(J_1, J_2 > 0)$ in the region $J_1 + J_2 > |J_\square|$ lying between two frustration planes (FP)

$$J_1 + J_2 = |J_\square|: \quad \text{FP} \tag{2}$$

the ground state of the model is SAF. A continuous transition from the paramagnetic (PM) to the SAF phase occurs at some critical temperature $T_c > 0$.

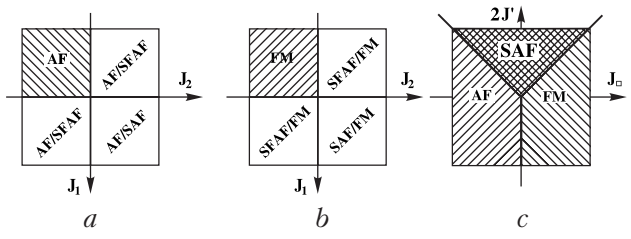

Fig. 3. Plane projections of the 3D diagram shown in Fig. 2. (*a*): Upper part $J_\square > 0$, view from the top. (*b*): Lower part $J_\square < 0$, view from the top. (*c*): Compactification of 3D Fig. 2 in the special case $J_1 = J_2 \equiv J'$ [8].

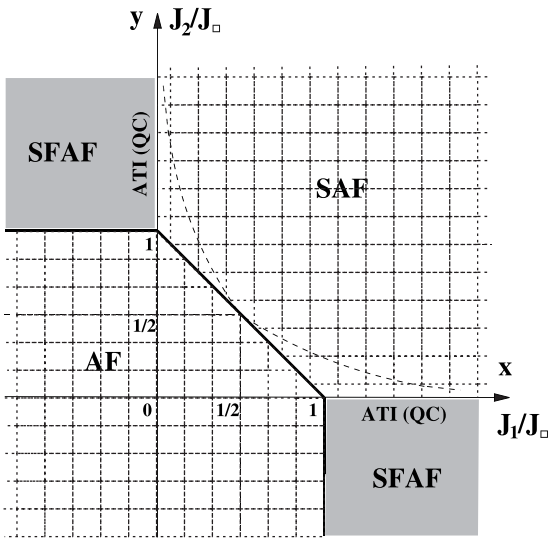

Fig. 4. Plane phase diagram for the ratios of the couplings, corresponding to the 3D Fig. 2 at $J_\square > 0$. The phase boundaries (thick solid lines) correspond to the frustrations planes FP and FP′ . The thick dashed lines (online) indicate the boundaries of the incommensurate global minima locus $(y > 1/2,\ x > 1/2,\ y < 1/4x)$ discussed in the text. The case $J_\square < 0$ can be obtained by the substitutions $J_{1,2}/J_\square \mapsto J_{1,2}/|J_\square|$, AF $\mapsto$ FM in this figure.

From the arguments known for the case $J_1 = J_2$ [12] (see also [13] for a more general symmetry analysis of the Ginzburg–Landau functional) this transition is non-universal: the critical indices continuously depend on the couplings $J_\square, J_1, J_2$.

In the region $J_1 > J_\square$ of the fourth quadrant $(J_1 > 0, J_2 < 0)$ lying between the other pair of frustration planes FP′

$$J_1 = |J_\square|: \quad \text{FP}' \tag{3}$$

the ground state is SFAF. The same arguments [12,13] suggest non-universality of the PM $\to$ SFAF transition.

In the regions lying above (beneath) the frustration planes FP and FP′, and above (beneath) the basal plane $J_\square = 0$ in the third quadrant, the ground state is a usual AF (FM), respectively. The transition PM $\to$ AF (FM) belongs to the 2D Ising universality class. The second quadrant $J_1 < 0, J_2 > 0$, not shown in Fig. 2, is obtained by a reflection over the plane $J_1 = J_2$. In the AF (FM) state the number of frustrated (diagonal) bonds per plaquette is two in the first quadrant, one in the second and the fourth, and zero in the third.

Transitions at finite temperature should be absent on the frustration planes FP/FP′ where the model is highly degenerate. We are not aware of studies of the ground state in these cases and cannot say at the moment whether the system possesses some kind of a

long-range order at zero temperature or not, except a rather trivial line $J_\square = J_1 = 0, J_2 < 0$ of the FP′ planes crossing where the model becomes a set of decoupled Ising chains, and four special lines on the FP planes where it becomes the exactly-solvable isotropic triangular Ising (ITI) model. The latter case will be discussed momentarily.

Exactly-solvable limits

In the 3D space $(J_1, J_2, J_\square)$ beside the frustration planes FP and FP′, there are three special planes where one of the couplings is zero. On these planes the model (1) reduces to the exactly solvable cases.

Let us start with the upper part $(J_\square > 0)$ of the SAF region

$$J_\square < J_1 + J_2 \ . \qquad (4)$$

On the SFAF–SAF boundary $J_2 = 0$ the model is equivalent to the anisotropic Ising model on a triangular lattice (ATI), for which exact results are available [14–17]. The antiferromagnetic $(J_\square, J_1 > 0)$ ATI model with one strong bond $J_1 > J_\square$ is disordered at any non-zero temperature [17]. It orders only at $T = 0$, i.e., it is quantum critical (QC). The highly degenerated ground state (however with a vanishing zero-temperature entropy per site) can be viewed as a 2D array of antiferromagnetically ordered (along the strong bond J_1) correlated chains. The oscillating (with a period of four lattice spacings) power-law decay of the spin-spin correlation function along $J_\square$-directions [17] indicate on the preference of the ferromagnetic order along the «missing» diagonal J_2. This resembles the SFAF state, however any couple of adjacent J_1-chains is uncorrelated. We label this state occurring on two sectors of the J_1(or J_2) $= 0$ planes as ATI (QC) on the phase diagram (Fig. 2). Since the critical behavior of the ATI model with two equal weak ferromagnetic bonds $|J_\square| < J_1$ is equivalent to the totally antiferromagnetic ATI model [17], the ATI (QC) state smoothly continues into the lower $(J_\square < 0)$ part of the SFAF-SAF boundary.

The sectors $J_2 = 0, J_1 > 0$ (and $1 \leftrightarrow 2$) above the FP $J_1 + J_2 = J_\square$ correspond to the antiferromagnetic ATI model with one weak bond $J_1 < J_\square$. It is known [17] to have only two phases and to order at finite temperature. $T_c(\mathrm{PM} \to \mathrm{AF})$ as a function of couplings is also known exactly. The sectors $J_2 = 0, J_1 < 0, J_\square > 0$ (and $1 \leftrightarrow 2$) correspond to the antiferromagnetic ATI model which is even not frustrated, and $T_c(\mathrm{PM} \to \mathrm{AF}) > 0$ at any $J_\square > 0$. The PM $\to$ AF transition in the ATI model belongs to the 2D Ising class. So, except the SFAF-SAF boundary, the ordered phase on the exactly-solvable «triangulation» planes J_1(or J_2) $= 0$ is the same as the AF ground state in the interior in this region of the phase diagram.

The situation on the «triangulation» planes in the lower part $(J_\square < 0)$ of the phase diagram is exactly analogous to the upper part, with an obvious replacement AF $\leftrightarrow$ FM.

Note that the ground states change on the lines where the triangulation and frustration planes cross. To put it differently, these are the lines of quantum phase transitions. The AF (FM) phase disappears in the limit $J_1 \to |J_\square| - 0$ $(J_2 = 0)$. Also, the zero-temperature AF in-chain order (ATI (QC)) described above disappears in the limit $J_1 \to |J_\square| + 0$ $(J_2 = 0)$ as well. The ITI model $J_1 = J_\square$ is disordered at any non-zero temperature (indicated as ITI (QC) in Fig. 2). Its ground state, albeit having finite entropy per site, possesses periodical (with a period of three lattice spacings) long-range order [16].

The basal plane $J_\square = 0$ in Fig. 2 corresponds to the case when Hamiltonian (1) represents two decoupled identical NN Ising models residing on two superimposed lattices (shown by circles and squares in Fig. 1). Diagonal couplings $J_{1,2}$ are the NN couplings of these Ising models. This is the only exactly-solvable limit (labelled by 2 × 2DI in Fig. 2) within the SFAF (or SAF) region of the phase diagram. In this limit the PM $\to$ SAF (or SFAF) phase transition enters into the 2D Ising universality class.

Incommensurate (floating) phase

So far we have discussed the ground-state phases of the model and the critical behavior on the boundaries of these phases with the disordered phase, as well as on the special planes (lines). However, there is also a possibility that ordering into the ground-state phases of Fig. 2 happens not necessarily from the PM phase, but from some other one(s) occurring at non-zero temperature. A very simple analysis indicates that this indeed can take place in our model. Fourier-transforming the Hamiltonian (1) we obtain (we set the lattice spacing to unity)

$$H = \sum_{\mathbf{q}} J(\mathbf{q}) T^x(\mathbf{q}) T^x(-\mathbf{q}) \ , \qquad (5)$$

$$J(\mathbf{q}) = J_\square(\cos q_x + \cos q_y) +$$

$$+ J_1 \cos(q_x - q_y) + J_2 \cos(q_x + q_y) \ ,$$

where $\mathbf{q}$ runs within the first Brillouin zone $|q_{x,y}| \le \pi$. At mean-field level, a minimum of $J(\mathbf{q})$ in $\mathbf{q}$-space defines the wave-vector $\mathbf{q}_0$ of the critical freezing mode $T^x(\mathbf{q}_0)$, i.e. the order parameter $\langle T^x_{\mathbf{m}} \rangle \propto \cos(\mathbf{q}_0 \mathbf{m} + \varphi)$ below a certain critical temperature T_c. In different regions $(J_1, J_2, J_\square)$ of the ground-state phase diagram (Fig. 2) we find mini-

mum at $\mathbf{q}^{F/A} = (0,0)/(\pi,\pi)$ giving the FM/AF order parameter and two minima $\mathbf{q}_{1,2}^{SAF} = (\pi,0)/(0,\pi)$ giving two components of the SAF order parameter. (The latter represent two possible ordering patterns of the SAF phase and via some transformation can be related to magnetizations of the superimposed sublattices [12].) The important point is that the positions of the *commensurate* (C) extrema $\mathbf{q}^{\sharp}$ ($\sharp$ = F, A, SAF) of $J(\mathbf{q})$ do not depend on couplings.

There are however two other pairs of extrema $\pm\mathbf{q}^{s,a}$ which exist if

$$|J_{\square}| < 2|J_1| \quad \text{and/or} \quad 2|J_2|\,. \tag{6}$$

These extrema lie on the diagonal of the Brillouin zone. $\mathbf{q}^{s,a}$ are generically *incommensurated* (IC) and depend on couplings as

$$q_x^s = -q_y^s = \arccos\left(-\frac{J_{\square}}{2J_2}\right), \tag{7}$$

$$q_x^a = -q_y^a = \arccos\left(-\frac{J_{\square}}{2J_1}\right). \tag{8}$$

In Fig. 5, we show the positions of all extrema of $J(\mathbf{q})$ within the Brillouin zone. In the SFAF ground state region (e.g., in the fourth quadrant $J_1 > 0, J_2 < 0$ shown in Fig. 2) the pair of extrema $\pm\mathbf{q}^a$ (8) gives global minima of $J(\mathbf{q})$ (the other pair of solutions (8) $\pm\mathbf{q}^s$ when exists, corresponds to its maxima), and $|q_x^a| = |q_y^a| > \pi/2$. As we see, two IC modes $\pm\mathbf{q}^a$ could give components of the SFAF ground state order parameter's wave vectors $\pm\mathbf{q}^{SFAF} = \pm(\pi/2,-\pi/2)$ only if $J_{\square} = 0$. (In the second quadrant of the SFAF region when $J_1 < 0, J_2 > 0$, the vectors $\mathbf{q}^s$ and $\mathbf{q}^a$ exchange their roles. Because of the $J_1 \leftrightarrow J_2$ symmetry, in the following we will always discuss the fourth quadrant for concreteness.)

The locus of the IC global minima does not coincide with the SFAF ground state region, but overlaps with the neighboring FM, AF, and SAF phases. The minimum $J(\pm\mathbf{q}^a)$ is located between two planes $|J_{\square}| = 2J_1$ in the fourth quadrant, and in two regions of the half of the first quadrant ($J_2 < J_1$): (i) between $J_{\square} = +2J_1$ and $J_{\square} = +2\sqrt{J_1 J_2}$; (ii) $+ \mapsto -$. The regions of the IC minima in the other half ($J_2 > J_1$) of the first quadrant (as in the second quadrant) are obtained from the described above by $J_1 \leftrightarrow J_2$, $\mathbf{q}^a \mapsto \mathbf{q}^s$. On the plane phase diagram shown in Fig. 4 this locus is restricted by the lines $y = 1/2$, $x = 1/2$, $y = 1/4x$, shown by the dashed lines.

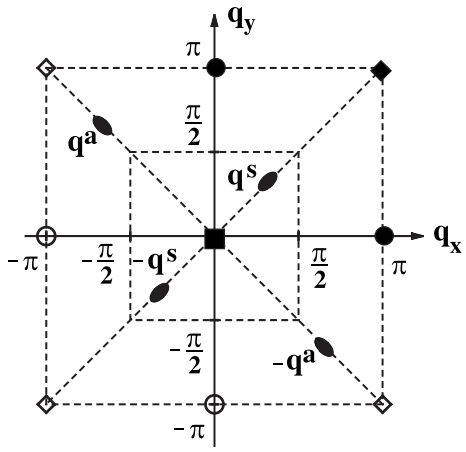

Fig. 5. Positions of extrema of $J(\mathbf{q})$ (5) in the Brillouin zone. Open symbols connected to their bold counterparts by a reciprocal lattice vector. Incommensurate extrema $\pm\mathbf{q}^{a,s}$ (7), (8) (shown for the case $J_1 > 0, J_2 < 0$) exist if conditions (6) are satisfied.

So we can conclude that at finite temperature the model possesses an IC phase and there is an IC–C phase transition where the IC wave vector $\mathbf{q}^a$ locks into one of the (commensurate) ground-state phase vectors. As in 2D the IC phase has only an algebraic long-range order, it is called floating [10]. The origin of the IC floating phase in our model is frustration (competing interactions). Such phase is well known from another example of frustrated Ising model, i.e., the ANNNI model which was intensively studied in the past [1,10,11]. In that model the floating phase locks into the antiphase which has the wave vector $\mathbf{q} = (0, \pi/2)$. (The antiphase is analogue of our SFAF phase.) The ANNNI model also provides an example showing that the mean-field (minimization) analysis does not work well in defining boundaries between the floating and commensurate phases in 2D, and the extend of the IC phase is less than the mean field suggests*.

We will not attempt to locate exactly the phase boundaries at finite temperature in this study. Following Domany et al. [13] in classification of the ordered phases by commensurability p, i.e., the ratio of superstructure's period and lattice spacing along a given direction, we can label the phases as follows: F $\mapsto 1 \times 1$; AF $\mapsto 2 \times 2$; SAF $\mapsto 1 \times 2$ (or 2×1); SFAF $\mapsto 4 \times 4$**. From mapping of the 2D IC-C phase transition to the Kosterlitz-Thouless problem, it is established that

* The well-studied ANNNI phase diagram with the FM and antiphase ground states [1,10,11] is an analogue of the lower part of the fourth quadrant (FM–SFAF) of our diagram in Fig. 2.

** According to this notation, the antiphase of the 2D ANNNI model is (1×4). For the same reasons we give for our case, the floating phase of that model exists only within the antiphase ground state region.

there is no such (continuous) transition for commensurate phases with small $p^2 < 8$ [10,18]. From this result with the proviso of continuity of phase transition(s) in the model, we conclude that the IC floating phase cannot «spill» beyond the SFAF ($p = 4$) ground-state region of the phase diagram, even if a naive (mean-field) analysis suggests that within the F, AF, and SAF regions there are some parts where it could be possible (see Fig. 4). The only high-temperature phase the latter three regions have a common border, is the disordered PM.

Combining this with the known exact critical properties of the model on the special planes discussed above, we end up with the qualitative finite-temperature phase diagram shown in Fig. 6. Since on the plane $J_\square = 0$ the model (1) is just two decoupled Ising lattices, the floating phase must be absent. Mean-field arguments suggest that the floating phase disappears exactly at $J_\square = 0$ giving rise to a Lifshitz point (L). Note that the floating phase does not appear if the diagonal couplings are equal even at the mean-field level (see Fig. 4), which agrees with known more sophisticated analyses of this case [1].

The model in transverse field

Now we turn to the analysis of the NN and NNN Ising Hamiltonian H (1) in the presence of a transverse field. The total Hamiltonian of the Ising model in transverse field (IMTF) reads

$$H_{\mathrm{IMTF}} = H - \Omega \sum_i \mathcal{T}_i^z \ . \qquad (9)$$

The Ising operators are normalized to satisfy the spin algebra

$$[\mathcal{T}_i^\alpha, \mathcal{T}_j^\beta] = i\delta_{ij}\varepsilon_{\alpha\beta\gamma}\mathcal{T}_i^\gamma \ . \qquad (10)$$

There is no exact solution of the transverse 2D Ising model even for the case of NN couplings only ($J_1 = J_2 = 0$). The ground state phase diagram of the Hamiltonian (9) can be analyzed from the known mapping of the d-dimensional IMTF at zero temperature onto the $(d+1)$-dimensional Ising model at a given (non-zero) «temperature» [3]. In our case the 2D NN and NNN IMTF maps onto the 3D Ising model comprised of the 2D layers (1) coupled *ferromagnetically* in the third (Trotter) direction with the coupling $J_T \propto -\ln\coth\Omega < 0$. For such (2 + 1)-dimensional model a mean-field analysis gives a qualitatively correct diagram of the *ground state* phases of the 2D IMTF [3]. The new coupling J_T does not bring any additional frustration to the 2D NN and NNN model. Analysis of $J_3(q_x, q_y, q_T) = J_T \cos q_T + J(q_x, q_y)$ where $J(q_x, q_y)$ is given by (5), shows that J_T does not modify the domains of the global minima in the $(J_1, J_2, J_\square)$-space, adding only a trivial $q_T = 0$ third component to the two-dimensional vectors $\mathbf{q}^\sharp$ discussed above (cf. Fig. 5.) The temperature phase diagram of the 3D Ising model with the spectrum $J_3(q_x, q_y, q_T)$ (if we label the phases according to the in-plane ordering pattern defined by the 2D vectors $\mathbf{q}^\sharp$) looks similar to that shown in Fig. 6, with one very important distinction: the above-mentioned argument related to phase's commensurability p does not apply in 3D, so the IC region is not restricted to lie above the SFAF phase, but can spill into the neighboring regions of the $(J_1, J_2, J_\square)$-space. From the mean-field arguments, the IC region is given by the locus of the IC minima $J(\pm\mathbf{q}^{a/s})$ defined in the previous section. So, the IC phase instead of being locked between the special planes FP′ and $J_2 = 0$ as shown in Fig. 6,*a* and *b*, respectively, can spread up to the locus boundaries shown by the crosses. From the equivalence between the zero-temperature d-dimensional IMTF (quantum Ising) and the $(d+1)$-dimensional classical Ising model, we infer that the ground-state phase diagram of the former on the plane $(\Omega/J, J_\sharp)$ should have the same structure as the described above $(T, J_\sharp)$ diagram of the latter. So we expect the transverse field to generate the IC ground-state phase not only in the SFAF region of the Ising coupling space, but also in the neighboring parts of the F, AF, and SAF regions. From minimization arguments the latter are restricted by the dashed lines on the plane diagram in Fig. 4 and by the crosses in Fig. 6.

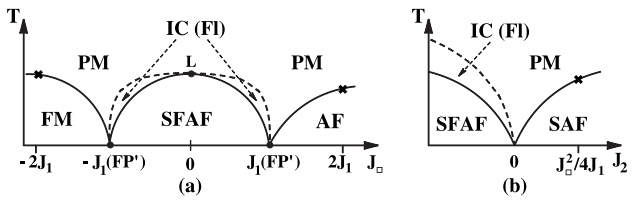

Fig. 6. Qualitative temperature phase diagram. The IC floating (Fl) phase lies beneath the dashed lines. Crosses indicate the borders of the IC minima locus. (*a*): For fixed $J_1 > 0$, $J_2 < 0$. On the plane $J_\square = 0$ the floating phase must be absent. We assume that it smoothly disappears at $J_\square = 0$ resulting in a Lifshitz point (L). (*b*): The same for fixed $J_1 > 0$, $|J_\square| < J_1$.

From analogies with the ANNNI model, we rather expect this «IC region» to be filled with infinitely many commensurate phases with different p [10,11], but detailed analysis of this question, as well as the full *finite-temperature* phase diagram of the transverse model (9) need a separate study.

In the rest of the paper we will be particularly interested in the SAF region of the coupling space, and restrict ourselves to the couplings

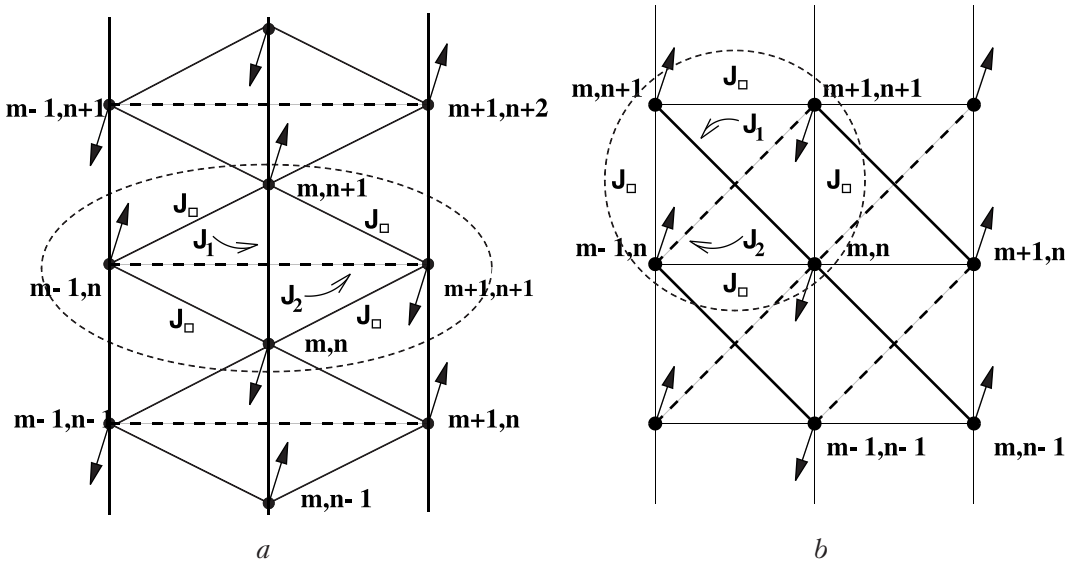

a *b*

Fig. 7. 2D effective lattice of coupled ladders. A vertical line and a represent dot a single ladder and its rung where pseudospin $\mathcal{T}_{mn}$ and spin $\mathbf{S}_{mn}$ (not shown) reside. In the region encircled by the dashed line the Ising couplings between pseudospins are indicated. Two pseudospins from $(m-1)$-th and $(m+1)$-th ladders are coupled not only by J_2 (bold dashed line), but also via the dimerization constant ε. The $\mathcal{T}^x_{mn}$-ordering pattern shown corresponds to the SAF phase (*a*). The same after mapping on a square lattice (*b*).

$$J_{\square}^2 < 4J_1J_2, \quad (J_1, J_2) > 0 \,. \tag{11}$$

According to Fig. 4, it means that we choose the couplings to lie above the hyperbole $y = 1/4x$. The first condition in (11) ensures that the couplings lie in the region where $\mathbf{q}_{1,2}^{\mathrm{SAF}} = (0,\pi)/(\pi,0)$ provide a global minimum of model's spectrum, so the phase with the IC solutions $\mathbf{q}^{a/s}$ does not intervene. The second in the above conditions stipulates that even if $J_{\square} = 0$ we stay away from the planes where our model becomes the triangular Ising. A transverse field can generate exotic temperature phases in that model. Such phases were found [4,5] in the particular case of the isotropic (antiferromagnetic) transverse triangular Ising model*.

From mapping between the quantum and classical Ising models we conclude that at zero temperature our IMTF with the couplings satisfying (11) possesses a single QCP which separates the SAF and PM ground state phases. The mean field predicts a two-phase PM/SAF diagram. The critical temperature T_c of the second-order PM–SAF phase transition evolves smoothly from the QCP $T_c(J/\Omega_{\mathrm{cr}}) = 0$ to the asymptotic limit $T_c(\infty)$ of the classical model (see dashed curve in Fig. 8, where $g \equiv (J_1 + J_2)/\Omega$). It is also known that the mean field gives a qualitatively correct phase diagram for the IMTF when $d \geq 2$ [3]. Thus we argue that the mean-field result shown by the dashed curve in Fig. 8 *does represent* the phase diagram of the IMTF (1), (9), (11), while its quantitative aspects, e.g., the exact value of the QCP, should be corrected via more accurate treatments.

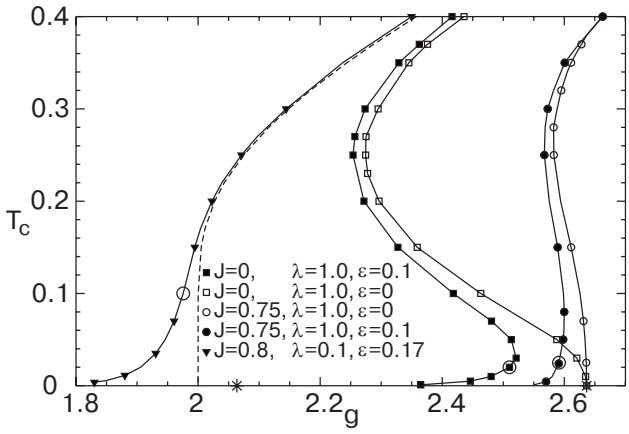

Fig. 8. Critical temperature of the PE-SAF phase transition as a function of the Ising coupling g at different values of J, λ, ε from the numerical solution of Eqs. (21). The dashed line corresponds to the pure IMTF ($J = \lambda = \varepsilon = 0$). Two stars on the abscissa show the positions of critical couplings $g_\lambda = 2.0627\ (2.6366)$ for $\lambda = 0.1\ (1.0)$, respectively. Large empty circles on the curves with $\varepsilon \neq 0$ indicate the right boundary of the exponential BCS regime (25). At large values of g (not shown) all curves $T_c(g)$ approach the asymptotic line $T_c = g/4$.

* By analogy with the triangular Ising case of Refs. 4, 5, we expect the transverse field to bring about new exotic phases near the frustration planes FP, FP′, where the ground state of our model is also infinitely degenerate.

3. Coupled spin-pseudospin model

Now we turn to the analysis of the IMTF (1), (9) coupled to the quantum spins **(S)** residing on the same sites of the lattice as the Ising spins do. The latter we will call *pseudospins* from now on. Such coupled spin-pseudospin (or spin-orbital) models emerge in various contexts, most notably the Jahn-Teller transition-metal compounds [19] or many kinds of low-dimensional quantum magnets. For a recent short overview and more references, see [6].

Models of the type we study in the present work appear in analysis of the quarter-filled ladder compound NaV_2O_5. The Hamiltonian of this material can be mapped onto a spin-pseudospin model with spins and pseudospins residing on the same rung of a ladder [20–22]. The ladders form a 2D lattice. The long-range pseudospin order $\langle T_i^x \rangle \neq 0$ represents physically the charge disproportionation between left/right sites on a rung below T_c.

This system was analyzed on the effective triangular lattice shown in Fig. 7,*a* by solid lines [20,22]. However, in the case of NaV_2O_5 the Ising couplings generated by Coulomb repulsion are antiferromagnetic and $J_1 > J_\square$. Since the triangular Ising model with one strong side is disordered [17], one needs an extra coupling (J_2-diagonal) to stabilize the observed SAF long-range order. In our earlier study [6] we explicitly took into account J_1, while the other diagonal J_2 was effectively generated via the spin-pseudospin coupling*.

In this work we take into account the Ising couplings $J_\square$, J_1, J_2 between neighboring sites of the effective lattice, as shown in Fig. 7,*a*. Then such effective lattice can be mapped onto the square lattice shown in Fig. 7,*b* with the NN and NNN Ising couplings. For NaV_2O_5 all $J_\sharp > 0$, so the model is frustrated. As follows from geometry of the original NaV_2O_5 lattice, J_2 is the weak diagonal and J_1 is the largest coupling:

$$J_2 < J_\square < J_1 \ . \tag{12}$$

We assume $J_\square$ to be small enough not only to lie beneath the frustration plane (2), but to satisfy a more stringent condition (11). Then according to the above analysis, the IMTF with these couplings has a two-phase (PE–SAF) diagram with a QCP**. In the literature on NaV_2O_5 its charge order is called the «zig-zag phase», what characterizes the antiferroelectric order in a *single ladder* only. In fact, the *two-dimensional long-range charge order* in NaV_2O_5 is SAF. For a detailed explanation of this point, including interpretation of the experimental crystallographic data on the charge order [23] in terms of the Ising pseudospins, see [24].

In the following we will work with dimensionless quantities: Hamiltonians $\mathcal{H} = H/\Omega$, temperature $T \to T/\Omega$ and Ising couplings $g_\sharp \equiv J_\sharp/\Omega$. With site labelling shown in Fig. 7, the IMTF Hamiltonian is:

$$\mathcal{H}_{\rm IMTF} = \sum_{m,n} \left\{ -\mathcal{T}^z_{mn} + \frac{1}{2}\left[g_\square \left(\mathcal{T}^x_{mn}\mathcal{T}^x_{m+1,n+1} + \mathcal{T}^x_{mn}x\mathcal{T}^x_{m+1,n} \right) + g_1 \mathcal{T}^x_{mn}\mathcal{T}^x_{m,n+1} + g_2 \mathcal{T}^x_{mn}\mathcal{T}^x_{m+2,n+1} \right] \right\} . \tag{13}$$

For the decoupled spin sector of the total Hamiltonian we take into account only the strongest coupling between spins on the NN rungs of a ladder. In terms of the effective lattice (cf. Fig. 7) this translates into a set of decoupled Heisenberg chains with the usual antiferromagnetic spin exchange J. These parallel chains are oriented along the J_1-diagonals.

As we infer from our previous work on a simpler version of the IMTF Hamiltonian [6], there are two spin-pseudospin interaction terms resulting in two qualitatively distinct aspects of model's criticality: the inter-ladder spin-pseudospin interaction $\propto \varepsilon$, and the in-ladder spin-pseudospin interaction $\propto \lambda$. The former, in terms of the equivalent square lattice, linear over difference of the charge displacement operators $\mathcal{T}^x$ on the NNN sites along the weak J_2-diagonal, is responsible for the simultaneous appearance of the SAF order and the spin gap, as well as for the destruction of the IMTF QCP***. The latter, quadratic over the NNN charge opera-

* A linear coupling $\propto \varphi(\mathcal{T}_1 \mp \mathcal{T}_2)$ with some Gaussian mode φ results in an effective anti-/ferrro-magnetic interaction between $\mathcal{T}_1$ and $\mathcal{T}_1$. Such terms can create or renormalize the couplings of the Ising effective Hamiltonian. In his context the Ising model with two NNN couplings of different signs is less academic than it might appear.

** Since in applications to NaV_2O_5 the Ising pseudospins $\mathcal{T}$ represent charge displacements, the appropriate names for the phases are «paraelectric» (PE) and «super-antiferrolelectric». We keep the same abbreviation SAF for the latter.

*** This type of coupling is allowed by the symmetry of the original NaV_2O_5 lattice [6]. Numerical estimates of ε from a microscopic Hamiltonian are given in [25]. Note also that ε effectively couples the spin chains.

tors along the J_1-diagonal, is responsible for the re-entrance. With all these terms the total effective Hamiltonian reads:

$$\mathcal{H} = \mathcal{H}_{\rm IMTF} + \sum_{m,n} \mathbf{S}_{mn}\mathbf{S}_{m,n+1}[J + \lambda\mathcal{T}^z_{m,n}\mathcal{T}^z_{m,n+1} + \varepsilon(\mathcal{T}^x_{m+1,n+1} - \mathcal{T}^x_{m-1,n})] \,. \tag{14}$$

The dimensionless couplings J, λ, ε in the Hamiltonian (14) are positive, and the spin operators satisfy the same algebra (10) as the pseudospins (while S and $\mathcal{T}$ commute). The sums above run through $1 \le m \le \mathcal{M}$ and $1 \le n \le \mathcal{N}$. For brevity we will use the notation $D_{mn} \equiv \mathbf{S}_{mn}\mathbf{S}_{m,n+1}$. In this study we consider the model with the XY spin sector:

$$D_{mn} = S^x_{mn}S^x_{m,n+1} + S^y_{mn}S^y_{m,n+1} \,. \tag{15}$$

The range of couplings under consideration will be restricted to

$$(J, \lambda) \lesssim g_1, \quad \varepsilon \lesssim \max J, \lambda \,. \tag{16}$$

Spin-SAF phase transition

We treat the Hamiltonian (14) following conventional wisdom of molecular-field approximations (MFA) [26]. In the present version of MFA the pseudospins are decoupled and averaged with the density matrix $\rho^{\mathcal{T}} \propto \exp(-\beta \mathbf{h}_{mn}\boldsymbol{\mathcal{T}}_{mn})$, where $\mathbf{h}_{mn}$ is the Weiss (molecular) field, while the spin sector is treated exactly via a Jordan-Wigner transformation. The details are presented in [6]. Similar to the pure IMTF with couplings (11) we assume the possibility of the SAF order in the coupled model (14). So we take the following Ansätze for the Ising pseudospin averages (i.e., the charge ordering parameters in terms of the real physical quantities)

$$\langle \mathcal{T}^z_{mn} \rangle = m_z \,, \tag{17}$$

$$\langle \mathcal{T}^x_{mn} \rangle = (-1)^{m+n} m_x \,. \tag{18}$$

It is easy to see from the Hamiltonian (14) that ansatz (18) creates a dimerization in the spin sector, therefore a natural assumption for the dimerization operator average is

$$\langle D_{mn} \rangle = -[t + (-1)^{m+n}\delta] \,. \tag{19}$$

With the new coupling

$$g \equiv g_1 + g_2 \tag{20}$$

the molecular-field equations and results derived in [6] for the case $g_2 = g_\square = 0$ (i.e., $g = g_1$) can be applied here. Some of them we reproduce in this paper in order to make it more self-contained, and for the use in what follows as well.

The average quantities are determined by the system of four coupled equations

$$m_z = \frac{1}{2}\frac{1 + 2\lambda t m_z}{\mathfrak{y}} \tanh\frac{\beta\mathfrak{y}}{2} \,, \tag{21a}$$

$$m_x = \frac{m_x}{2}\frac{g + 2\varepsilon\eta}{\mathfrak{y}} \tanh\frac{\beta\mathfrak{y}}{2} \,, \tag{21b}$$

$$t = \frac{1}{\pi}\int_0^{\pi/2} d\varphi \, \frac{\cos^2\varphi}{\xi(\varphi)} \tanh\tilde{\beta}\xi(\varphi) \equiv \frac{1}{\pi} t_n(\Delta, \tilde{\beta}) \,, \tag{21c}$$

$$\eta = \frac{\Delta}{\pi m_x}\int_0^{\pi/2} d\varphi \, \frac{\sin^2\varphi}{\xi(\varphi)} \tanh\tilde{\beta}\xi(\varphi) \equiv \frac{\Delta}{\pi m_x}\eta_n(\Delta, \tilde{\beta}) \,, \tag{21d}$$

where $\mathfrak{y} = \sqrt{h_x^2 + h_z^2}$ is the absolute value of the Ising molecular field

$$h_z = 1 + 2\lambda t m_z \,, \tag{22a}$$

$$h_x = g m_x + 2\varepsilon\delta \,. \tag{22b}$$

The other auxiliary parameters are defined as follows:

$$\delta \equiv m_x \eta \,, \tag{23a}$$

$$\xi(\varphi) \equiv \sqrt{\cos^2\varphi + \Delta^2 \sin^2\varphi} \,, \tag{23b}$$

$$\Delta \equiv \frac{2\varepsilon m_x}{J + \lambda m_z^2} \,, \tag{23c}$$

$$\tilde{\beta} \equiv \frac{\beta}{2}(J + \lambda m_z^2) \,. \tag{23d}$$

At some critical temperature T_c the coupled model undergoes the phase transition. It is of the second kind, with the thermodynamic behavior of the physical quantities as the Landau theory of phase transitions predicts [6]. With the spin-pseudospin (-charge) coupling ε present, the SAF charge order $m_x \neq 0$ and the spin gap $\Delta_{\rm SG} = 2\varepsilon m_x$ appear simultaneously below T_c. By analogy with the spin-Peierls transition, when the Peierls phonon instability (freezing) creates the spin gap, it is natural to call this type of transition the *spin-super-antiferroelectric (spin-SAF)* transition.

It is worth to point out an important property of the Hamiltonian (14): in the other domains of Ising couplings (not considered in our analysis of the coupled model) where the Ising sector of (14) can order into, e.g., FM, AF, or SFAF phase, the dimerization (gap) in the spin sector does not occur.

The behavior of $T_c(g)$ in the coupled model (14) shows two new striking features comparatively to the pure IMTF: re-entrance and destruction of the QCP

[6]. In the absence of the spin-charge coupling ε, the model (14) has a QCP at

$$g_\lambda \equiv 2\left(1+\frac{\lambda}{\pi}\right), \tag{24}$$

where T_c vanishes (see Fig. 8). λ renormalizes the QCP comparatively to the pure IMTF value $g=2$. The coupling ε, responsible for the spin gap generation also destroys the QCP, resulting in the exponential behavior of T_c in the region $g \le g_\lambda$, where the model would have been disordered at any temperature if $\varepsilon = 0$. This constitutes an important feedback from the spins on the charge degrees of freedom, allowing the very possibility of the model *to order at all.* Approximate analytical solutions for $T_c(g)$ in the regimes of strong Ising couplings and the BCS- are: [6]

$$T_c \approx \begin{cases} \dfrac{g}{4}, & g >> g_\lambda\ , \\ \dfrac{\mathbb{A}\tilde{J}}{2}\exp\left[-\dfrac{\pi\tilde{J}}{4\varepsilon^2}(g_\lambda - g)\right], & \text{BCS regime}\ , \end{cases} \tag{25}$$

where $\mathbb{A} \equiv 8/[\pi \exp(1-\gamma)] \approx 1.6685$, $\gamma \approx 0.5772$ is Euler's constant, and

$$\tilde{J} \equiv J + \frac{\lambda}{4}\ . \tag{26}$$

The boundary where the low-temperature BCS regime sets in and the related formulas are applicable, is given approximately by the condition

$$\text{BCS regime:}\ \ g < g_\lambda + \frac{4\varepsilon^2}{\pi\tilde{J}}\ . \tag{27}$$

The BCS regime has many analogies with the standard theory of superconductivity, apart from the exponential dependence of T_c on couplings. In particular, several physical quantities (order parameter, BCS ratio, specific heat jump) manifest certain «universal» behavior near T_c, similar to that known from the BCS theory [6].

Another particularity of $T_c(g)$ found earlier [6] from the numerical solution of Eqs. (21), is re-entrance in the intermediate regime $g \sim g_\lambda$. The re-entrance occurs in the coupled model with the QCP ($\varepsilon = 0$), while when $\varepsilon \neq 0$ the critical temperature can even manifest a double re-entrant behavior before it reaches the BCS regime (see Fig. 8). A detailed analysis of the coupled model in the regime of re-entrance was not done previously. We will address this in the next subsection, mainly analytically, in order to get more insight on the underlying physics and, in particular, to establish conditions when the re-entrance can occur.

Re-entrance

Let us first reproduce some earlier formulas [6] for reader's convenience. At $T \le T_c$ one equation from the pair (21a,b) can be written in a form

$$m_z^{-1} = g + \frac{4\varepsilon^2}{\pi(J+\lambda m_z^2)}\eta_n - \frac{2\lambda}{\pi}t_n,\ \ T \le T_c\ . \tag{28}$$

At $T = T_c$ we have Eqs. (21a) as

$$m_z = \frac{1}{2}\tanh\frac{\beta_c}{2}\left(1+\frac{2\lambda m_z}{\pi}t_n\right), \tag{29}$$

and parameters t_n, η_n are given by Eqs.(21c,d) with $\Delta = 0$. The latter two functions have the following expansions: [6]

$$t_n(0,x) \approx \begin{cases} \dfrac{\pi}{4}x\left(1-\dfrac{1}{4}x^2\right) + \mathcal{O}(x^5),\ x<1\ , \\ 1 - \dfrac{\pi^2}{24}\dfrac{1}{x^2} + \mathcal{O}(1/x^4),\ \ x>1\ , \end{cases} \tag{30}$$

and

$$\eta_n(0,x) \approx \begin{cases} \dfrac{\pi}{4}x\left(1-\dfrac{1}{12}x^2\right) + \mathcal{O}(x^5),\ \ \ x<1\ , \\ \ln\mathbb{A}x + \dfrac{\pi^2}{48}\dfrac{1}{x^2} + \mathcal{O}(1/x^4),\ x>1\ . \end{cases} \tag{31}$$

Case $\varepsilon = 0$; re-entrance with QCP

As one can easily see from Eqs. (28), (29) there is no re-entrance when $\lambda = 0$. This is a well-known fact for the pure IMTF, as on the mean-field level, as well as beyond MFA [3,26]. To study the re-entrance analytically and in particular, to establish whether there is some minimal value of λ when it appears, we should distinguish between two asymptotic regimes of the mean-field equations. Let us first consider the regime (it can occur only if $\tilde{J} < 1$) when ($T_c \equiv 1/\beta_c$)

$$\frac{1}{2}\tilde{J} < T_c < \frac{1}{2}\ . \tag{32}$$

(In all regimes of couplings the re-entrance occurs at $T_c < 1/2$.) By carrying out the leading-term expansions of the functions in Eqs. (28), (29) we obtain

$$g = 2 + 4\exp(-1/T_c) + \frac{\lambda\tilde{J}}{4T_c} \tag{33}$$

for a single-valued function $g(T_c)$. The non-monotonic (i.e., re-entrant) behavior of $T_c(g)$ is related to the existence of an extremum of $g(T_c)$. The coupling $g_{\min}$ which defines the minimal value of g for the order in m_x being possible (in the pure IMTF with $\lambda = 0$ this was the QCP), and in the same time the left border of the re-entrant region

$$g_{\min} < g < g_\lambda \,, \tag{34}$$

is defined from the minimum of the function $g(T_c)$ (33). This point corresponds to the critical temperature

$$T_* = \ln^{-1} \kappa_\circ, \quad \kappa_\circ \equiv \frac{16}{\lambda \tilde{J}} \tag{35}$$

for which

$$g_{\min} \approx 2 + \frac{4}{\kappa_\circ}(1 + \ln \kappa_\circ) \,. \tag{36}$$

The consistency of the solution (35) with (32) implies the condition

$$2 < \ln \kappa_\circ < \frac{2}{\tilde{J}} \,. \tag{37}$$

The other regime corresponds to the case when

$$T_c < \min \{1/2, \tilde{J}/2\} \,. \tag{38}$$

Proceeding in the same way as above, we obtain for $g(T_c)$ in this case:

$$g = g_\lambda + 4 \exp(-g_\lambda/2T_c) - \frac{\lambda\pi}{3\tilde{J}^2} T_c^2 \,. \tag{39}$$

Let us point out that the conditions (32), (38) determine two different regimes ($x < 1$ or $x > 1$) of the asymptotics (30), (31) we apply in order to obtain $g(T_c)$ as (33) or (39). So if $\tilde{J} < 1$ there are regions of T_c where condition (32) is satisfied, then the approximation (33) applies. However at sufficiently low temperatures ($T_c < \tilde{J}/2$) we inevitably enter the other regime (38) where the asymptotics (30), (31) change ($x < 1 \mapsto x > 1$), and the function $g(T_c)$ crosses over from (33) to (39). If, on the contrary, $\tilde{J}$ is large, then condition (32) never applies, and the approximation (39) describes the whole region $T_c < 1/2$.

Extrema T_* of the function $g(T_c)$ (39) are determined by the transcendental equation

$$\exp(-g_\lambda/2T_*) = \frac{\lambda\pi}{3g_\lambda \tilde{J}^2} T_*^3 \,. \tag{40}$$

This equation always has a trivial solution $T_*' = 0$ corresponding to the (local) maximum of $g(T_c)$. This is the QCP, and the curve $T_c(g)$ approaches the QCP normally to the abscissa (see Fig. 8). Two non-trivial solutions of (40) exist if the couplings satisfy the condition

$$\tilde{J} > \mathbb{C}_1 \lambda^{1/2} g_\lambda \,, \tag{41}$$

where

$$\mathbb{C}_1 \equiv \sqrt{\frac{\pi}{24}\left(\frac{e}{3}\right)^3} \approx 0.3121 \,. \tag{42}$$

There is only one solution within the validity region of the approximation (39), and it corresponds to the minimum of $g(T_c)$. If the couplings satisfy (41) then

$$u \equiv \ln 3 + \frac{1}{3}\ln a_\circ > 1 \,, \tag{43}$$

$$a_\circ \equiv \frac{24\tilde{J}^2}{\pi\lambda g_\lambda^2} \,,$$

and the minimum can be found analytically as

$$T_* \approx \frac{g_\lambda}{6}\left(\frac{1}{u} - \frac{\ln u}{u^2}\right). \tag{44}$$

For the left border of the re-entrant region we obtain

$$g_{\min} = g_\lambda - \frac{\lambda\pi}{3\tilde{J}^2} T_*^2 + \frac{4\lambda\pi}{3g_\lambda \tilde{J}^2} T_*^3 \,. \tag{45}$$

The above equations agree well with the numerical solutions of the MFA (21) at different values of couplings (from comparison of the asymptotics (33), (39) and the numerical curves at various couplings and temperatures we found the deviations $\sim 5\%$ at most). More importantly, the analytical results of this subsection allows us to understand in details the interplay of the scales provided by model's couplings and the temperature, resulting in the re-entrance. Let us explain this on the example of two characteristic numerical curves shown in Fig. 8.

The curve shown for $J = 0, \lambda = 1, \varepsilon = 0$ ($\tilde{J} = 0.25$) corresponds to the case of small $\tilde{J}$. At $T_c \gtrsim \tilde{J}/2 = 0.125$ it is well described by the equations for the regime (32). Its re-entrant behavior and, in particular, the minimum $g_{\min}$ is due to the last term on the r.h.s. of (33). At lower temperatures $T_c \lesssim 0.125$ the asymptotics (33) is not applicable, the curve is described by (39). Note that since $\mathbb{C}_1 \lambda^{1/2} g_\lambda \approx 0.8229$, the condition (41) for the minimum is broken, and the asymptotics (39) describes the featureless low-temperature evolution of this curve towards the maximum at the QCP.

The second curve in Fig. 8 with $J = 0.75, \lambda = 1, \varepsilon = 0$ ($\tilde{J} = 1$) corresponds to the case of large $\tilde{J}$. The whole re-entrant region ($T_c < 0.4$), including the position of the minimum $g_{\min}$ ($\mathbb{C}_1 \lambda^{1/2} g_\lambda \approx 0.8229$) is described by the interplay of the last two terms on the r.h.s. of Eq. (39). Comparison of Eqs. (36), (45) allows also to understand a more pronounced re-entrant behavior for the case of smaller J.

As we see from our analysis of Eqs. (33), (39) in the both regimes (32), (38), the re-entrant behavior on the phase diagram occurs at any $\lambda \neq 0$.

Case $\varepsilon \neq 0$; double re-entrance, no QCP

The absence of re-entrance at $\lambda = 0$ can be proven rigorously. Indeed, combining Eqs.(28), (29) we obtain the equation

$$m_z^{-1} = g + \frac{4\varepsilon^2}{\pi J}\eta_n\left(0, \frac{J}{2}\ln\frac{1+2m_z}{1-2m_z}\right) \qquad (46)$$

which has one and only one solution $m_z \in [0, 1/2]$ for a given value of g. This solution in its turn provides a unique value of T_c via Eq. (29), thus no re-entrance.

At $\lambda \neq 0$ continuous evolution of $T_c(g)$ between the regimes of strong Ising coupling and BCS (cf. Eq. (25)) can occur either with a double re-entrance (i.e., with one minimum and one maximum of $g(T_c)$) within the re-entrant region

$$g_{\min} < g < g_{\max} , \qquad (47)$$

or without re-entrance. In the latter case the function $T_c(g)$ (or $g(T_c)$) has only an inflexion point (see Fig. (8)).

Following the analysis given in the previous subsection, we obtain for the case of small $\tilde{J}$ in the regime (32)

$$g = 2 + 4\exp(-1/T_c) + \frac{\lambda\tilde{J} - 2\varepsilon^2}{4T_c} . \qquad (48)$$

Again, the re-entrant behavior is conditioned by the existence of a minimum of $g(T_c)$. It exists if, at least

$$\varepsilon < \frac{1}{\sqrt{2}}\sqrt{\lambda\tilde{J}} \approx 0.7071\sqrt{\lambda\tilde{J}} . \qquad (49)$$

The unique minimum of $g(T_c)$ (48) defines the left border of the re-entrance region $g_{\min}$ and corresponds to the critical temperature T_* given by Eqs. (35), (36) with $\kappa_\circ \mapsto \kappa$, and

$$\kappa \equiv \frac{16}{\lambda\tilde{J} - 2\varepsilon^2} . \qquad (50)$$

The consistency imposes the constraint analogous to (37), more stringent than the «minimal requirement» (49).

The other regime (38) is described by the approximation

$$g = g_\lambda + 4\exp(-g_\lambda/2T_c) - \\ - \frac{\pi T_c^2}{3\tilde{J}^3}(\lambda\tilde{J} + \varepsilon^2) - \frac{4\varepsilon^2}{\pi\tilde{J}}\ln\frac{\mathbb{A}\tilde{J}}{2T_c} . \qquad (51)$$

As we have explained in the previous subsection for the case $\varepsilon = 0$, the asymptotics (48) is applicable only for small $\tilde{J}$ at the intermediate temperatures (32), while (51) can be applied at arbitrary low temperatures, including the BCS region. The latter, given by the exponential dependence in (25), can be recovered if we retain only the first and last (leading) terms on the r.h.s. of Eq. (51).

In the regime (38) the re-entrance occurs if the equation for extrema of (51)

$$\exp(-g_\lambda/2T_*) = \frac{\pi T_*}{3g_\lambda\tilde{J}^3}\left[(\lambda\tilde{J} + \varepsilon^2)T_*^2 - \frac{6\varepsilon^2\tilde{J}^2}{\pi^2}\right] \qquad (52)$$

has non-trivial solutions. Note in making comparison of Eq. (52) to its counterpart (40) at $\varepsilon = 0$, that coupling ε destroys the QCP [6], as immediately seen from (51). So the trivial solution $T_* = 0$ of Eq. (52) corresponds to the unphysical singularity of g. As follows from (52), (38), non-trivial solutions are possible if, at least

$$\varepsilon < \frac{\pi}{2\sqrt{6}}\frac{1}{\sqrt{1 - \pi^2/24}}\sqrt{\lambda\tilde{J}} \approx 0.8357\sqrt{\lambda\tilde{J}} . \qquad (53)$$

If this condition is satisfied, the transcendental equation (52) has at least one solution, corresponding to maximum of $g(T_c)$. To leading order in ε, it occurs at the temperature

$$T_*' \approx \frac{\sqrt{6}}{\pi}\left(\frac{\tilde{J}}{\lambda}\right)^{1/2}\varepsilon \qquad (54)$$

and the coupling

$$g_{\max} \approx g_\lambda - \frac{4\varepsilon^2}{\pi\tilde{J}}\ln\frac{\mathbb{A}\pi\sqrt{\lambda\tilde{J}}}{2\sqrt{6}\varepsilon} . \qquad (55)$$

If the couplings meet both the conditions (41) and

$$\varepsilon < \mathbb{C}_2 g_\lambda\left(\frac{\lambda}{\tilde{J}}\right)^{1/2} , \qquad (56)$$

where

$$\mathbb{C}_2 \equiv \frac{\pi}{2}\sqrt{\frac{47 - 13\sqrt{13}}{36}} \approx 0.0936 , \qquad (57)$$

then a second solution of (52) (T_*''), corresponding to minimum of $g(T_c)$ exists. This minimum, located between

$$T_*' < T_*'' < \frac{g_\lambda}{6} \qquad (58)$$

is given approximately by Eq. (44) where u in (43) is modified by $a_\circ \mapsto a$, and

$$a \equiv \frac{24\tilde{J}^3}{\pi g_\lambda^2(\lambda\tilde{J} + \varepsilon^2)} . \qquad (59)$$

For validity of expansion (44) we assume $u > 1$.

The analytical results of this subsection allows us to describe the behavior of the coupled model at $\varepsilon \neq 0$, following from the MFA equations (21), both qualitatively and quantitatively. In Fig. 8 two counterparts ($\varepsilon = 0.1$) of the numerical curves discussed in the previous subsection are shown. For this case of small ε, re-entrance is possible, according to conditions (49), (53). The re-entrant behavior at the temperatures $T_c \gtrsim T_*'$ is not modified essentially by the presence of new coupling ε comparatively to the case $\varepsilon = 0$, and is in fact controlled by couplings J, λ, g. Since we have already discussed it in detail for the case $\varepsilon = 0$, we will not dwell on it any more. In the low-temperature regime (51) coupling ε changes drastically the behavior of $g(T_c)$ at $T_c \lesssim T_*'$, creating a maximum at $g(T_*')$ described well by the approximation (54) and turning $g(T_c)$ away from the QCP towards the BCS region. For the BCS regime Eq. (25) provides a virtually exact solution.

As follows from the inequalities (49), (53), (56) an increase of ε can suppress the re-entrance even at $\lambda \neq 0$. The necessary conditions (49), (53) for extrema of the two asymptotics (48), (51) are close, albeit with a rather small mismatch of the coefficient. Conditions for re-entrance are more stringent, since they require the consistency between the solutions for extrema and the validity ranges of the appropriate asymptotics. The (overrated) critical value $\varepsilon_\circ \sim 0.7\sqrt{\lambda \tilde{J}}$ gives a good simple estimate for the boundary where the re-entrance disappears from the whole curve $g(T_c)$, whether $\tilde{J} > 1$ or $\tilde{J} < 1$. An example of the curve $T_c(g)$ without re-entrance is shown in Fig. 8.

To summarize our analysis of the re-entrance for the cases $\varepsilon = 0$ and $\varepsilon \neq 0$: it reveals the robustness of this phenomenon in the coupled model (14) and its underlying mechanism, namely, competition between different scales defined by the couplings $J, \lambda, \varepsilon, g$ and the temperature. These competing scales (interactions) are not related to the Ising frustration which is present in the model as well ($(J_\square, J_1, J_2) > 0$), since the latter is not accounted for explicitly by our mean-field equations. This competing mechanism for the re-entrance appears to be robust and not being an artifact of the MFA. Re-entrant phases due to competing interactions are known also, e.g., from exact solution of the Ising model on the union-jack lattice [27], or from analyses of decorated Ising models [28].

It is not clear for us at the moment how the proposed re-entrance can be observed. NaV_2O_5 is, up-to-date, the only known compound with the spin-SAF transition and does not show re-entrance. This is in agreement with our estimates for the parameters for the effective Hamiltonian for this compound. They give its g located on the disordered side of the (destroyed) QCP, and the re-entrance on the whole curve $T_c(g)$ would be only very weak (i.e., localized near $g \sim g_\lambda$), if any. It appears experimentally that, e.g., external pressure cannot modify the in-plane parameters of NaV_2O_5 strongly enough, such that re-entrance would be generated. The variations of the interlayer couplings under pressure, on the other hand, generate various types of order (including devil's staircase) with regard to the plane stacking, while the in-plane SAF order remains unaffected [24,29].

4. Summary and discussion

We study the 2D Ising model on a square lattice with nearest-neighbor ($J_\square$) and non-equal next-nearest neighbor ($J_{1,2}$) interactions. The cases of classical and quantum models are considered.

We find the ground state phase diagram of the classical Ising model at arbitrary $J_\square, J_1, J_2$. Along with the three ordered phases — ferromagnetic, antiferromagnetic, and SAF — known for $J_1 = J_2$ [8], in a more general case $J_1 \neq J_2$ there is a region of the coupling space with the super-ferro-antiferromagnetic (or (4×4)) ground state phase and an incommensurate phase at finite temperature, not reported before. The three phases — SAF, SFAF, IC — can occur only in the presence of competing interactions (frustrations) on the Ising model's plaquette.

A particularly interesting conclusion from the analysis of the quantum model's phase boundaries is that transverse field Ω can stabilize the IC ground-state phase (located for $\Omega = 0$ in the region with sign $(J_1/J_2) = -1$) in some parts of the AF and SAF regions of the coupling space where $(J_1, J_2) > 0$, but $J_1 \neq J_2$. These regions, along with vicinities of the special planes of degeneracy (triangulation and frustration) in coupling space, are good candidates for the quantum model to demonstrate a very non-trivial critical behavior. Leaving this for a future work, we hope that our findings will inspire additional interest in this model. Taking into account only one simple example of a mapping shown in Fig. 7, it is clear the model with $J_1 \neq J_2$ is not so exotic.

We analyze the IMTF coupled to the XY spin chains in the restricted (SAF) region of $(J_\square, J_1, J_2)$ where the IMTF has a simple two-phase (disordered-SAF) diagram with a QCP, similar to that of the transverse NN model. Our interest in this model is motivated by the problem of the phase transition in the quarter-filled ladder compound NaV_2O_5. The predictions of the mean-field equations for the critical properties of the coupled spin-pseudospin model do not differ essentially from our earlier results for a simpler Hamiltonian [6]. Due to the spin-pseudospin cou-

pling ε, the QCP of the NN and NNN IMTF is destroyed, and in the whole SAF region (11) of Ising couplings the spin-pseudospin model undergoes the spin-SAF transition. We should point out, that albeit the exponential BCS regime (25) on the disordered side of the IMTF QCP $g < g_\lambda$ formally extends up to $g = 0$, decreasing g, i.e. $J_1 + J_2$, will eventually remove us from the coupling region (11) where the SAF pseudospin solution of the MFA equations is applicable.

We perform a detailed analytical study of re-entrance in the coupled model. In particular, we establish the conditions when it can occur. The analytical results not only agree well with the direct numerical calculations in various regimes, but allows us to understand the physical mechanism of re-entrance due to interplay of competing interactions in the coupled model.

In this work we gain more insights on the transition in the spin-pseudospin model, and we can sharpen our previous statements concerning the applications to NaV_2O_5 [6]. The present analysis of Ising sector allows us to identify the 2D long-range charge order in that compound as the SAF phase. As follows from known results on the ordering of the frustrated 2D Ising model into the SAF phase [1], the spin-SAF transition has non-universal coupling-dependent critical indices. Experiments indicate rather wide regions of the two-dimensional structural (charge-ordering) fluctuations characterized by the critical index $\beta \approx$ $\approx 0.17-0.19$ [30–32], close to $\beta = 1/8$ of the 2D Ising model. Due to known difficulties in extracting critical indices from experimental data, it seems problematic to diagnose the deviations from universality caused by $0 < J_\square/J_1 < 1$. (Note that in the limit $J_\square$ the PM-SAF transition enters into the 2D Ising universality class, and for NaV_2O_5, due to its geometry, the ratio $J_\square/J_1$ should be small.)

On the theory side, the critical indices of the PM-SAF transition as functions of couplings in the NN and NNN Ising model have been calculated by various methods only at $J_1 = J_2$ [1]. The critical exponents are unknown for the case $J_1 \neq J_2$, and it appears to be an interesting problem to study.

Another very interesting issue we addressed recently in a separate study [24], is the 3D nature of the transition in NaV_2O_5. According to the correlation lengths measurements [30], upon approaching $T_c = 34$ K the 2D crossover of the pretransitional structural fluctuations occurs somewhere at $T \sim 50$ K. The model considered in the present work deals with a single plane, leaving aside the question of charge ordering along the third (stacking) direction. The phase transition in NaV_2O_5 quadruples the unit cell in the stacking direction, and the recent x-ray experiments, carried out deep in the ordered phase [23,33] revealed peculiar stacking ordering patterns of the super-antiferroelectrically charge-ordered planes. In addition, the pressure can change these patterns and even generate a multitude of higher-order commensurate superstructures in the stacking direction (devil's staircase) [29]. To explain these phenomena we proposed a 3D extension of the Ising sector with additional competing couplings between the nearest and next-nearest planes [24]. In the limit $J_\square$ the Ising sector reduces to two identical interpenetrating decoupled 3D ANNNI models. Although inclusion of the competing interlayer couplings accommodates the explanation for the observed stacking charge order in the framework of the spin-SAF (in-plane) mechanism of the transition in NaV_2O_5, a deeper understanding of the critical properties of a very complicated model with the 3D Ising sector warrants a further work.

We are grateful to D.I. Khomskii, E. Orignac, and P.N. Timonin for helpful discussions. This work is supported by the German Science Foundation. G.Y.C. also acknowledges support from a LURF grant.

1. R. Liebmann, *Statistical Mechanics of Periodic Frustrated Ising Systems*, Springer, Berlin (1986).
2. S. Sachdev, *Quantum Phase Transitions*, Cambridge University Press, Cambridge (1999).
3. B.K. Chakrabarti, A. Dutta, and P. Sen, *Quantum Ising Phases and Transitions in Transverse Ising Models*, Springer, Berlin (1996).
4. R. Moessner and S.L. Sondhi, *Phys. Rev.* **B63**, 224401 (2001).
5. M.V. Mostovoy, D.I. Khomskii, J. Knoester, and N.V. Prokof'ev, *Phys. Rev. Lett.* **90**, 147203 (2003).
6. G.Y. Chitov and C. Gros, *Phys. Rev.* **B69**, 104423 (2004).
7. P. Lemmens, G. Güntherodt, and C. Gros, *Phys. Rept.* **375**, 1 (2003).
8. C. Fan and F.Y. Wu, *Phys. Rev.* **179**, 560 (1969).
9. Such state, with the name of (4×4) superstructure was described before, e.g., by D.P. Landau and K. Binder, *Phys. Rev.* **B31**, 5946 (1985). It can also occur in the 2D Ising model where along with NN and NNN, the third-neighbor interactions are included.
10. P. Bak, *Rep. Prog. Phys.* **45**, 587 (1982).
11. W. Selke, *Phys. Rep.* **170**, 213 (1988).
12. S. Krinsky and D. Mukamel, *Phys. Rev.* **B16**, 2313 (1977).
13. E. Domany, M. Schick, J.S. Walker, and R.B. Griffiths, *Phys. Rev.* **B18**, 2209 (1978).
14. G.H. Wannier, *Phys. Rev.* **79**, 357 (1950); Errata: *Phys. Rev.* **B7**, 5017 (1973).
15. R.M. F. Houtappel, *Physica* **16**, 425 (1950).
16. J. Stephenson, *J. Math. Phys.* **11**, 413 (1970).
17. J. Stephenson, *J. Math. Phys.* **11**, 420 (1970).

18. S.N. Coppersmith, D.S. Fisher, B.I. Halperin, P.A. Lee, and W.F. Brinkman, *Phys. Rev.* **B25**, 349 (1982); *Phys. Rev. Lett.* **46**, 549 (1981); Erratum: *Phys. Rev. Lett.* **46**, 869 (1981).
19. K.I. Kugel and D.I. Khomskii, *Usp. Fiz. Nauk* **136**, 621 (1982) [*Sov. Phys. Usp.* **25**, 231 (1982)].
20. M.V. Mostovoy and D.I. Khomskii, *Solid State Commun.* **113**, 159 (1999).
21. D. Sa and C. Gros, *Eur. Phys. J.* **B18**, 421 (2000).
22. M.V. Mostovoy, D.I. Khomskii, and J. Knoester, *Phys. Rev.* **B65**, 064412 (2002).
23. S. Grenier, A. Toader, J.E. Lorenzo, Y. Joly, B. Grenier, S. Ravy, L.P. Regnault, H. Renevier, J.Y. Henry, J. Jegoudez, and A. Revcolevschi, *Phys. Rev.* **B65**, 180101(R) (2002).
24. G.Y. Chitov and C. Gros, *J. Phys.: Condens. Matter* **16**, L415 (2004).
25. C. Gros and G.Y. Chitov, *Europhys. Lett.* **69**, 447 (2005).
26. R. Blinc and B. ekš, *Soft Modes in Ferroelectrics and Antiferroelectrics*, North-Holland Publishing Co., Amsterdam (1974).
27. V.G. Vaks, A.I. Larkin, and Y.N. Ovchinnikov, *Zh. Eksp. Teor. Fiz.* **49**, 1180 (1965) [*Sov. Phys. JETP* **22**, 820 (1966)].
28. E.H. Fradkin and T.P. Eggarter, *Phys. Rev.* **A14**, 495 (1976).
29. K. Ohwada, Y. Fujii, N. Takesue, M. Isobe, Y. Ueda, H. Nakao, Y. Wakabayashi, Y. Murakami, K. Ito, Y. Amemiya, H. Fujihisa, K. Aoki, T. Shobu, Y. Noda, and N. Ikeda, *Phys. Rev. Lett.* **87**, 086402 (2001).
30. S. Ravy, J. Jegoudez, and A. Revcolevschi, *Phys. Rev.* **B59**, 681 (1999).
31. B.D. Gaulin, M.D. Lumsden, R.K. Kremer, M.A. Lumsden, and H. Dabkowska, *Phys. Rev. Lett.* **84**, 3446 (2000).
32. Y. Fagot-Revurat, M. Mehring, and R.K. Kremer, *Phys. Rev. Lett.* **84**, 4176 (2000).
33. S. van Smaalen, P. Daniels, L. Palatinus, and R.K. Kremer, *Phys. Rev.* **B65**, 060101 (2002).